

An unusual timing and spectral state of a black hole microquasar XTE J1550–564 *

Ying-Kang Jin¹, Shuang-Nan Zhang^{2,3} and Ti-Pei Li^{1,2,3}

¹ Department of Engineering Physics and Center for Astrophysics, Tsinghua University, Beijing 100084, China, jinyingkang@tsinghua.org.cn

² Department of Physics and Center for Astrophysics, Tsinghua University, Beijing 100084, China

³ Key Laboratory of Particle Astrophysics, Institute of High Energy Physics, Chinese Academy of Sciences, Beijing 100049, China

Received 2007 December 4; accepted 2008 October 10

Abstract An unusual timing and spectral state of a black hole microquasar XTE J1550–564 observed with RXTE is analyzed. Millisecond variabilities are found, which are significantly shorter than the minimum possible time scale in the light curves of black hole binaries, as suggested by Sunyaev & Revnivtsev (2000). The X-ray spectral fitting result indicates that there is an unusual soft component in the spectrum, which may be responsible for the millisecond variabilities. The millisecond variabilities as well as the unusual soft spectral component should be produced from some small, but independent active regions in the accretion disk.

Key words: methods: data analysis — X-rays: binaries — X-rays: individual (XTE J1550–564)

1 INTRODUCTION

XTE J1550–564 was discovered by the All-Sky Monitor (ASM) on the *Rossi X-ray Timing Explorer* (RXTE) on September 7, 1998 (Smith 2000). It is a microquasar (Hannikainen et al. 2001; Corbel et al. 2002) hosting a black hole (BH) of $10.5 \pm 1.0 M_{\odot}$ (Orosz et al. 2002). XTE J1550–564 is an X-ray transient, and showed a series of strong outbursts in 1998–1999 (Sobczak et al. 1999; Homan et al. 2001), 2000 (Tomsick et al. 2001a; Rodriguez et al. 2003), 2001 (Tomsick et al. 2001b), 2002 (Belloni et al. 2002) and 2003 (Dubath et al. 2003). In 2000 April–June, XTE J1550–564 showed a ~ 70 day outburst. The spectral evolution indicated that this source transitioned from an initial low hard state (LS) to an intermediate state (IS) and then went back to the LS (Rodriguez et al. 2003).

Here we report an unusual state of XTE J1550–564 on 2000–05–06, when the source was in its intermediate state. The timing analysis results show that the characteristic time scale of the variability is shorter than the typical characteristic time scale of BH binary variabilities; the widths of X-ray shots span times of 1 ms and shorter. The energy spectral analysis results indicate that there is a significant soft component in the X-ray spectrum of this observation, which may be responsible for the millisecond variabilities.

Short time scale X-ray variability of accreting X-ray binaries is an important clue to understanding the emission processes and the nature of the compact objects in X-ray binary systems. Sunyaev and Revnivtsev (2000) analyzed the Fourier power spectra of some accreting Neutron Star (NS) binaries

* Supported by the National Natural Science Foundation of China.

and BH binaries in the low/hard spectral state. They noticed that the power spectra of NS binaries with a weak magnetic field contain significant power at frequencies close to 1 kHz, whereas for most BH binaries, the Fourier power spectra decline rapidly at frequencies higher than 10–50 Hz. This observed difference was explained as a result of the different region where the radiation of accreting NS binaries and BH binaries is produced. In the case of an accreting BH, all the observed radiation is produced either in an accretion disk, its corona or an advection flow. In the case of a NS, a significant part of the total energy should be released in the boundary layer or a layer of spreading matter on the surface of the NS (see Sunyaev & Revnivtsev 2000 for the details of the discussion about the radiation region and the highest possible frequency variabilities). Sunyaev & Revnivtsev (2000) concluded that the maximum possible frequency is 100 ~ 200 Hz for BH binaries and higher than several kHz for NS binaries. Not every NS binary shows variabilities at frequencies close to 1 kHz, since NS binaries in the high/soft state may lack high frequency variabilities; whereas for BH binaries, the absence of high frequency (higher than 1 kHz) variabilities should be shown in all spectral states.

Time scale spectra calculated directly in the time domain, using the time scale analysis technique developed by Li (2001), can also be used to study high frequency (short time scale) variabilities. For example, the power density spectrum (PDS) in the time domain (Li & Muraki 2002) and the w spectra (Feng, Li & Zhang 2004) have been proposed and used to study hard X-ray shots in X-ray binaries. Previous results from these studies indicated that the characteristic time scale of hard X-ray shots is about 0.1 s and the shortest width of shots is about 0.05 s for accreting BH binaries (see Li & Muraki 2002; Feng, Li & Zhang 2004), whereas the widths of X-ray shots span times of 1 ms or shorter for accreting NS binaries. These results are consistent with the results obtained from their Fourier power spectra.

In several BH X-ray binaries, high-frequency quasi-periodic oscillations (HFQPOs) have been detected. The oscillation frequencies are from 40 Hz to 450 Hz, near the Keplerian frequency on the last stable orbit (Remillard & McClintock 2006), and they are the highest frequency observed in variabilities of BH binaries so far. These oscillations are possibly driven by some type of resonance condition (Abramowicz & Kluzniak 2001). In the 2000 outburst of XTE J1550–564, HFQPOs at 180 ~ 270 Hz have been found (Miller et al. 2001).

In Section 2, the observations and the data used are introduced. In Section 3 we briefly introduce the timing analysis, and show the very short time scale variabilities in the light curves of this source. The energy spectral analysis and results are discussed in Section 4. In Section 5, we summarize the results and discuss a possible interpretation of the above results.

2 OBSERVATIONS

The observation of the unusual state was made with PCA/RXTE on 2000–05–06, with the observation ID 50134–02–06–00. The light curves and the X-ray spectrum are extracted using the HEADAS package version 6.1.2. The data are selected when the source was observed at an elevation angle larger than 10° and the offset pointing was less than 0.02° . Light curves used for short time scale timing analysis are binned to 0.25 ms extracted from the SB model data (2–13 keV). The X-ray spectrum is extracted from the Standard-2 model data (2–60 keV). In addition, we analyze an observation of this source (XTE J1550–564) with the observation ID 30188–06–03–00, which has a typical temporal spectra of BH binaries (Li & Muraki 2002; Feng, Li & Zhang 2004). The observations and other information are listed in Table 1.

3 TIMING ANALYSIS AND RESULTS

3.1 Temporal Spectra Methods

Li & Muraki (2002) proposed the power spectrum and the PDS in the time domain for a light curve $x(k)$ as

$$P(\Delta t) = \frac{\text{Var}(x)}{(\Delta t)^2} = \frac{(1/N) \sum_{k=1}^N [x(k) - \bar{x}]^2}{(\Delta t)^2}, \quad (1)$$

Table 1 PCA/*RXTE* Observations Used

Observation ID	Observation date	Band (keV)	Used in
50134–02–06–00	2000–05–06	2–5	Fig. 7
		6–13	Fig. 7
		2–13	Figs. 1–5
30188–06–03–00	1998–09–08	2–13	Figs. 1–2
50134–02–03–01	2000–05–01	2–60	Fig. 5

and

$$p(\Delta t) = \frac{dP(\Delta t)}{d\Delta t}, \quad (2)$$

where the light curve $x(k)$, $k = 1, \dots, N$, is a counting series with a time step Δt , and $\bar{x} = \sum_{k=1}^N x(k)/N$ is the average of the counts. The comparison between the Fourier PDS (PDS in the frequency domain) and the time-domain PDS can be used to reveal the characteristic time scale of the variabilities in a detected light curve. The Fourier PDS is significantly lower than the corresponding time-domain PDS when the time scale is shorter than the characteristic time scale of a stochastic process (see Li & Muraki 2002 for details of the method and the main results).

A w spectrum is defined as the differential coefficient of the mean absolute difference of an observed light curve. For a light curve $r(j; \delta t)$ where $r(j; \delta t)$ is the counting rate during the time interval $[j\delta t, (j+1)\delta t]$ and δt is the time resolution, first the light curve on time scale $\Delta t = M\delta t$ is given by

$$r_m(i; \Delta t) = \frac{1}{M} \sum_{j=iM+m}^{(i+1)M+m-1} r(j; \delta t), \quad (3)$$

where $i = 0, 1, \dots, N-1$ and $m \in [0, M-1]$ is the discrete phase of the time series. Then, the mean absolute difference of the light curve of Δt is defined as

$$W(\Delta t) = \frac{1}{M} \sum_{m=0}^{M-1} \left[\frac{1}{N-1} \sum_{i=0}^{N-2} \frac{|x_m(i+1; \Delta t) - x_m(i; \Delta t)|}{\Delta t} \right], \quad (4)$$

and finally, the w spectrum on time scale Δt is given by

$$w(\Delta t) = -\frac{dW(\Delta t)}{d\Delta t} \quad (5)$$

(see Feng, Li & Zhang 2004 for details of the method). A w spectrum is a probe of the lower cut-off time scale of X-ray shots from the light curves; it shows a cut-off at the time scale which indicates the shortest width of the X-ray shots.

These methods have been used to analyze some accreting BH binaries and NS binaries. For BH binaries, the Fourier PDS are significantly lower than the corresponding time-based PDS at the time scale shorter than about 0.1 s, whereas for NS binaries, the two PDS are generally consistent with each other. The w spectra of accreting BH binaries show a cut-off at the time scale near 0.05 s, but the w spectra of accreting NS binaries have no obvious cut-off above 0.01 s. These results indicate that the characteristic time scale and the shortest widths of shots are different between the variabilities of accreting BH binaries and NS binaries. For BH binaries, the variabilities have a characteristic time scale of 0.1 s, and the shortest width of shots is about 0.05 s. The typical PDS and w spectra for BH binaries (Li & Muraki 2002; Feng, Li & Zhang 2004) are very similar to that shown in Figure 1 (right panel) and Figure 2 (right panel) for an observation of XTE J1550–564 with the observation ID 30188–06–03–00. For NS binaries, the time scale of variabilities span times of 1 ms and shorter.

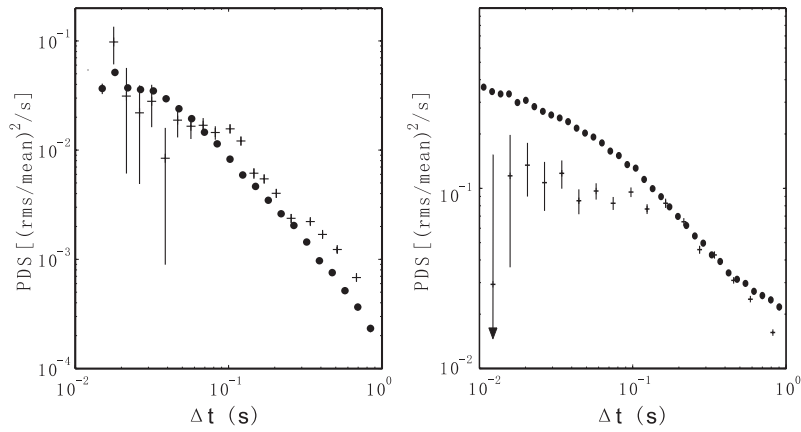


Fig. 1 Power density spectra. *Dot*: Time-based PDS. *Plus*: Fourier PDS. *Left panel*: the PDS of the observation of XTE J1550–564 on 2000–05–06. There are no significant differences between the Fourier PDS and the time-based PDS when the time scale is larger than 0.02 s, indicating that the characteristic time scale in this variability is not larger than 0.02 s. *Right panel*: the PDS of XTE J1550–564 with observation ID 30188–06–03–00, which is very similar to the typical PDS of BH binaries (Li & Muraki 2002). It is clear that the Fourier PDS is significantly lower than the time-based PDS when the time scale is shorter than 0.1 s.

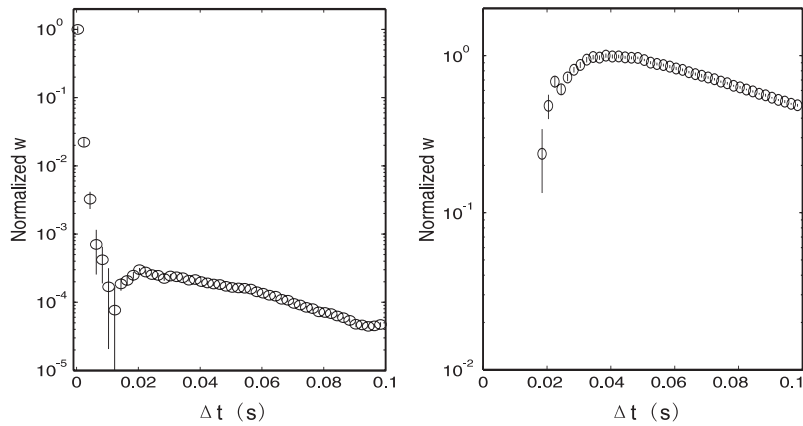


Fig. 2 w spectra. *Left panel*: the w spectrum of the observation of XTE J1550–564 on 2000–05–06. There are significant w spectrum signals at the time scale from 1 ms to 0.1 s, indicating that there are millisecond variabilities in this observation. *Right panel*: w spectrum of XTE J1550–564 with observation ID 30188–06–03–00, very similar to the typical w spectrum of BH binaries (Feng, Li & Zhang 2004). The w spectrum shows an obvious cut-off at about 0.02 s.

3.2 Results: Millisecond Variabilities

The temporal spectra methods are applied to the light curves of the observation on 2000–05–06. The light curves are binned to 0.25 ms for studying short time scale variabilities. The left panel of Figure 1 shows the PDS of the light curve extracted from this observation. The PDS of XTE J1550–564 with observation with ID 30188–06–03–00 is shown in the right panel of Figure 1 for comparison. Figure 2 shows the w spectra of these two observations. The PDS and w spectra of the observation with ID 30188–

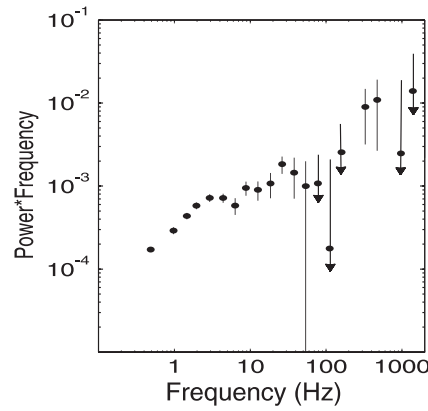


Fig. 3 Fourier power spectrum of the observation of XTE J1550–564 on 2000–05–06. The spectrum shows a decline at ~ 50 Hz. However, some power still exists at some frequencies close to 1 kHz.

06–03–00 are very similar to the typical PDS and w spectra for BH binaries (Li & Muraki 2002; Feng, Li & Zhang 2004). The results indicate that the characteristic time scale of the variability observed on 2000–05–06 is about 0.02 s, and the shortest width of shots span a time of 1 ms, which is much shorter than the typical time scales of BH binaries. The Fourier power spectrum is also obtained, as shown in Figure 3. The spectrum does show a decline at ~ 50 Hz; however some power still exists at some frequencies (not all frequencies) close to 1 kHz.

Since the millisecond variability in a BH binary is peculiar, further analysis is carried out. The relationship between rms (root-mean-squares) and flux at very short time scales in this observation is tested. The light curve binned to 0.25 ms is divided into many segments; in each segment there are 100 bins. The flux of every segment is obtained and binned. The rms of every segment is calculated, and $(\text{rms})^2$ of the segments in the same flux bin are averaged. The conventional method is to average rms of the segments in the same flux bin and take \sqrt{F} as the estimation of rms caused by Poisson noise, where F is the average flux (e.g., Zhang 2006); however, we caution that for a Poisson series $\langle \text{rms} \rangle$ is not an unbiased estimator of \sqrt{F} , whereas $\langle (\text{rms})^2 \rangle$ is an unbiased estimator of F . The conventional method is appropriate only when the number of bins is large enough (see Appendix A for details). If the $(\text{rms})^2$ of a time series at a certain time scale is obviously larger than the flux, the rms should be caused by not only the Poisson fluctuation, but also the variabilities in this time series at this time scale. The relationship between $(\text{rms})^2$ and flux in the observation of XTE J1550–564 is shown in the left panel of Figure 4. It is clear that the $(\text{rms})^2$ in this observation is obviously larger than the flux (the lines in Fig. 4 denote the relationship $(\text{rms})^2 = \text{flux}$), indicating the existence of millisecond variabilities.

3.3 Are they HFQPOs?

In the 2000 outburst of XTE J1550–564, the HFQPOs have been found as high as 270 Hz (Miller et al. 2001). To investigate the relationship between these HFQPOs and the millisecond variabilities found on 2000–05–06, we simulate a light curve containing QPOs with the frequency 250 Hz, FWHM 50 Hz and rms 10% (typical values for the HFQPOs reported in Miller et al. 2001). The w spectrum of this simulated lightcurve is calculated at time scales of several milliseconds, as shown in Figure 5, compared with the w spectrum of XTE J1550–564 on 2000–05–06 with the same time scales. The w spectrum of the HFQPOs light curve reaches its peak at a time scale of about 2 ms (half of the periods of the light curve, see Feng, Li & Zhang 2004 for details about the w spectrum of periodic series) and declines to negative (“cut off” when using logarithmic axis) when the time scale is shorter than 1.5 ms, while the w spectrum of XTE J1550–564 on 2000–05–06 is always positive at time scales shorter than 1 ms. In

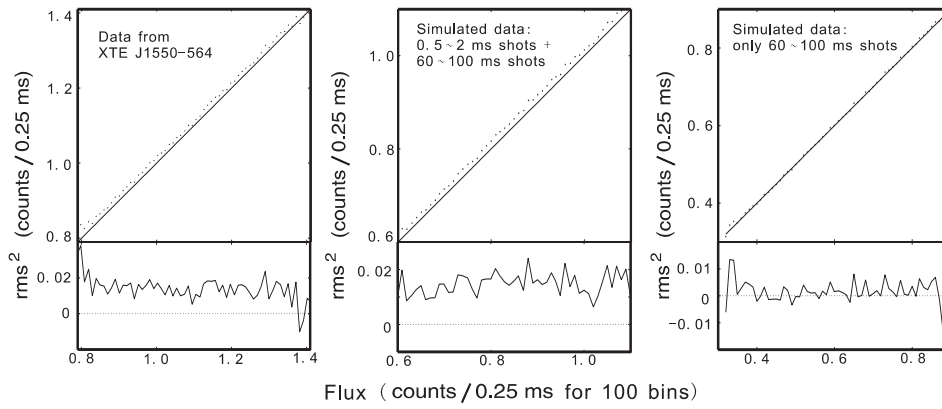


Fig. 4 Relationship between $(\text{rms})^2$ and flux of the X-ray light curve of XTE J1550–564 on 2000–05–06 and the simulated light curves. *Top panels:* Dots are for rms. Lines are for $(\text{rms})^2 = \text{flux}$, which means the rms are caused by Poisson fluctuation. *Bottom panels:* Lines are for rms with the Poisson noise removed. Dotted lines are for $(\text{rms})^2 = \text{flux}$. In the observed light curve (left panel) and the simulated light curve containing milliseconds shots (middle panel), the rms are obviously larger than the Poisson fluctuation. In the simulated light curve without millisecond shots (right panel), the rms are caused by the Poisson fluctuation. This is evidence of the existence of millisecond variabilities.

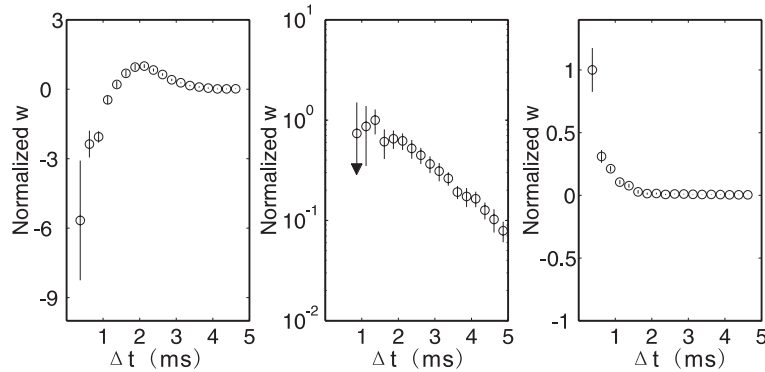


Fig. 5 *Left panel:* w spectrum of the simulated HFQPOs light curve with frequency 250 Hz, FWHM 50 Hz and rms 10%. *Middle panel:* w spectrum of the variability of XTE J1550–564 on 2000–05–01, in which HFQPOs of 261 Hz was reported. *Right panel:* w spectrum of the variability of XTE J1550–564 on 2000–05–06, in which no HFQPOs are detectable in its FFT power spectrum.

addition, the w spectrum of XTE J1550–564 on 2000–05–01 (Observation ID 50134–02–03–01, where HFQPOs at 261 Hz have been reported, see Miller et al. 2001) is obtained, and it is similar to the w spectrum of the simulated light curve. This result suggests that the HFQPOs observed in the 2000 outburst of XTE J1550–564 may contribute to some millisecond variabilities; however, the very short time scale variabilities (shorter than 1 ms) reported here should not be mainly caused by these HFQPOs.

4 ENERGY SPECTRAL ANALYSIS AND RESULTS

The X-ray spectrum of this observation is constructed from the PCA data with HEADAS 6.1.2. Since there is a ~ 100 s long flare which occurred mainly in 6–15 keV in this observation (see the discussion

in Sect. 5), the spectrum is extracted without the data when the flare occurred. Several models are tested to fit it using XSPEC 11.3.2. We do the fitting with the PCA data in energy bands between 2.5 and 25.0 keV. 2% systemic errors are added to the data in channels below 20 (about 8 keV) and 1% systemic errors are added to the data in channels above 20. The hydrogen column density value N_{H} is fixed to be $1.0 \times 10^{22} \text{cm}^{-2}$ according to *Chandra* observations (Kaaret et al. 2003). The multicolor disk blackbody plus a power law model, which is usually used to fit the X-ray spectrum of accreting BH binaries, cannot fit the data well (see the top left panel of Fig. 6). Some other models which contain two components are also tested. These models also fail to fit the data, especially the data around 2.5 keV. An additional very soft component is needed to fit the data. Adding a blackbody or a bremsstrahlung improves the fits significantly (see the bottom panels of Fig. 6). The null hypothesis probabilities of accepting the models are 0.218 (for adding a blackbody component) and 0.321 (for adding a bremsstrahlung component) respectively, thus the probability of accepting the bremsstrahlung model and refusing the blackbody model is only about 0.251, indicating that there is no strong support to accept one of them rather than the other one. All the models tested and the fitting results are listed in Table 2.

Table 2 Models tested to fit the X-ray spectrum and the results.

Model ^a	T_{in}^{b} (keV)	Photon Index	kT^{c} (keV)	CompTT			χ^2 (dof)	Flux ^d
				T0 (keV)	kT (keV)	τ_{up}		
I+II	0.90 ± 0.01	2.19 ± 0.01	333.6(46)	...
I+III	0.92 ± 0.01	0.13 ± 5.71	45.91 ± 1105.80	0.55 ± 22.69	360.7(44)	...
IV+II	...	2.09 ± 0.02	1.57 ± 0.02	162.9(46)	...
IV+III	1.59 ± 0.04	0.1 ± 5.40	52.16 ± 1324.37	0.55 ± 23.77	169.0(44)	...
V+I+II	1.14 ± 0.02	2.05 ± 0.02	0.35 ± 0.02	51.0(44)	1.9
IV+I+II	1.16 ± 0.03	2.05 ± 0.02	0.57 ± 0.04	47.8(44)	2.1

[a] I for diskbb, II for powerlaw, III for CompTT, IV for brems, V for blackbody. The prefix “wabs()” is omitted.

[b] Inner disk temperature and parameter for diskbb model.

[c] Temperature, parameter for brems model or blackbody model.

[d] The observed 1–60 keV flux (in units of $10^{-8} \text{ erg cm}^{-2} \text{ s}^{-1}$).

The fitting results therefore indicate that in this observation, there is an additional soft component besides the spectral components which are normally observed in BH binaries. Consequently, we suggest that the millisecond variabilities shown in the last section are somehow related to the very soft component in the spectrum.

To strengthen the above result, the w spectra of the light curves in two energy bands (2–5 keV and 6–13 keV) are obtained, as shown in Figure 7, and the results are compared with the w spectra of two simulated light curves, as shown in Figure 8. The simulated light curves are made of simulated shots and Poisson noise. For each light curve, the time resolution is 0.25 ms and the total duration is 1000 s. One light curve (in the left panel in Fig. 8) consists of shots whose widths are from 0.5 to 2.0 ms. The other light curve (in the right panel in Fig. 8) consists of two components of shots whose widths are from 0.5 to 2.0 ms and from 60 to 100 ms respectively. The w spectrum of the light curve in 2–5 keV is very similar to that of the simulated light curve made of only ~ 1 ms shots. The w spectrum of the light curve in 6–13 keV is similar to that of the simulated light curve made of two components of shots. The “cut-off” like w spectra at about 0.02 s should be caused by the component of shots whose widths are from 60 to 100 ms, and the significant w spectra at the time scale shorter than 0.01 s should be the contribution of the component of ~ 1 ms shots. These results verify the relationship between the millisecond variabilities and the unusual soft component in the spectrum, and thus we suggest that the millisecond variabilities are caused by the additional soft spectral component.

The relationship between rms and flux in the two simulated light curves are also tested, as shown in the middle and right panels of Figure 4. The $(\text{rms})^2$ in the simulated light curve consisting of millisecond

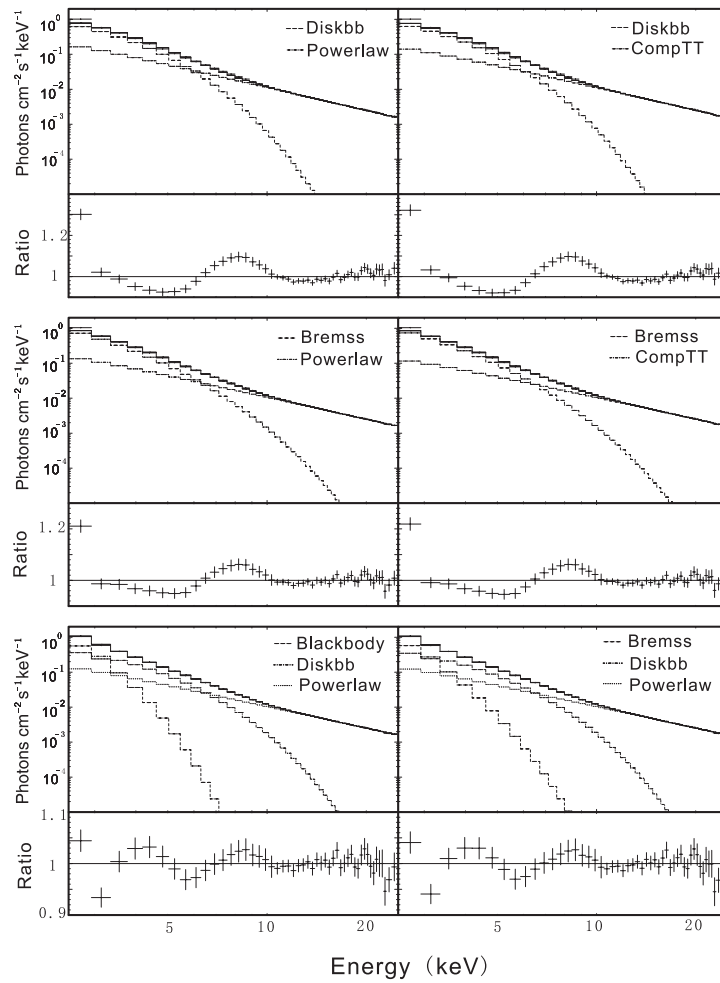


Fig. 6 PCA (2.5–25 keV) unfolded spectra and the corresponding ratios between models and data of XTE J1550–564 on 2000–05–06. The top two panels and middle two panels show the models which contain two components. These four models cannot fit the data well. The bottom two panels show the models with an additional soft component. These two fittings are more reliable.

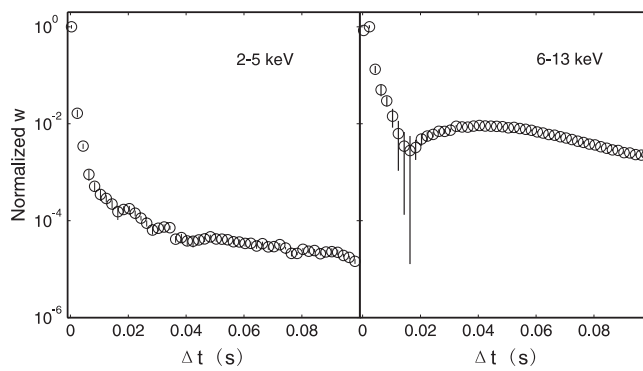


Fig. 7 w spectra of the variabilities in 2–5 keV and 6–13 keV of XTE J1550–564 on 2000–05–06.

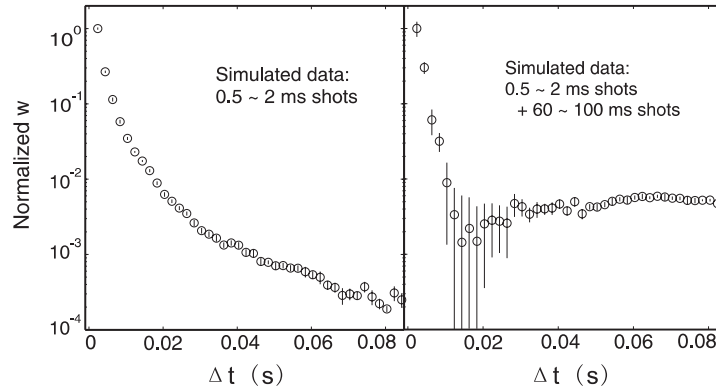


Fig. 8 w spectra of the simulated light curves.

shots (middle panel in Fig. 4) is obviously larger than the flux (the lines in Fig. 4 denote the relationship $(\text{rms})^2 = \text{flux}$), and the $(\text{rms})^2$ in the simulated light curve without millisecond shots (right panel in Fig. 4) is almost the same as the flux. These results also support existence for millisecond variabilities in this observation.

5 SUMMARY & DISCUSSION

The X-ray variability of the BH binary XTE J1550–564 on 2000–05–06 was studied using the temporal PDS and the w spectra. Very short time scale variabilities (one millisecond and shorter) were found in the variability. The time-based and Fourier power spectra of the variability were calculated. The power signals detected at short timescales or some frequencies close to 1 kHz verify the existence of the millisecond variabilities. The rms-flux relationship of the variability was obtained. The rms is obviously greater than the Poisson fluctuation, showing that the rms is partly caused by the millisecond variabilities. We investigated if the HFQPOs observed in the 2000 outburst of XTE J1550–564 may result in the w spectra and power signals near 1 ms. We conclude that the obvious difference between the w spectra of the simulated HFQPOs light curve and the variabilities of 2000–05–06 shows that the very short time scale variabilities reported here are not mainly caused by the HFQPOs.

The X-ray spectrum of this observation was studied. The spectral fitting results indicate that, in this observation, there is an additional soft component besides the multicolor disk model and the power law model which are normally used to fit the X-ray spectra of most BHs. This unusual soft component may be responsible for the millisecond variabilities, and this possibility is supported by the w spectra of the light curves in different energy bands and the simulated light curves. The PCA data of the energy band below 5 keV do not have sufficient information to distinguish which fit result of the different models is more reliable for this soft component, whose nature is difficult to determine. The very short time scale of the variability related to this soft component may indicate that the radiation region where this soft component occurs should be unusually small.

In Sunyaev & Revnivtsev (2000), the shortest possible time scale of variability in BH binaries has been discussed. The Keplerian frequency of the last stable orbit (about 100~200 Hz for Schwarzschild BHs $\sim 10 M_{\odot}$, and higher for Kerr BHs) was expected to be the maximal possible frequency for the variabilities of BH binaries. Thus, the very short time scale variabilities (shorter than 1 ms) in XTE J1550–564 are peculiar. Since the typical time scales of the instabilities which originated in the accretion disk (for example, the dynamical time scale, the thermal time scale) are all much longer than 1 ms, as discussed in Sunyaev & Revnivtsev (2000), we suggest that the millisecond variabilities should not be the result of any holistic behavior of the accretion disk; maybe they are dominated by the radiation from some individual active regions in the disk.

Uttley et al. (2005) have shown that the X-ray flux fluctuation of Cyg X-1 (characterized by rms of its flux) is proportional to its mean flux. Zhang (2006) discussed the similar rms-flux linearity phenomena in X-ray variabilities of solar flares and a gamma-ray burst. Such an rms-flux linearity indicates that the dynamical process for the X-ray production should be a non-linear “multiplicative” process rather than an additive process. The rms-flux relationship in this observation is shown in Figure 4. The rms with the Poisson fluctuation removed, which shows the flux fluctuation caused by the millisecond variabilities, remains almost constant when the flux increases (see left bottom panel of Fig. 4). It is different from the rms-flux linearity dominated by a non-linear “multiplicative” process, but very similar to the rms-flux relationship in the simulated light curve constructed by adding individual shots and overall noise (see middle bottom panel of Fig. 4). Therefore, we propose that the millisecond variabilities should be the result of the addition of some individual fluctuations caused by radiation from individual active regions.

In summary, unusually short time scale variabilities and additional soft spectral components are found in the BH binary XTE J1550–564 on 2000–05–06, and they should be produced from some small, but independent, active regions in the accretion disk.

Acknowledgements We thank Dr. Jian Hu of Tsinghua University for helpful discussions. This study is supported in part by the Ministry of Education of China, the Directional Research Project of the Chinese Academy of Sciences under project No. KJCX2-YW-T03, and the National Natural Science Foundation of China under project No. 10521001.

Appendix A: ESTIMATING THE POISSON NOISE IN THE RMS-FLUX RELATION

For counts series $x(i)$ ($i = 1, 2, \dots, m$) under a Poisson process with parameter λ , the $(\text{rms})^2$ is given by

$$\begin{aligned}
 (\text{rms})^2 &= \frac{1}{m-1} \sum_{i=1}^m \left(x_i - \frac{x_1 + x_2 + \dots + x_m}{m} \right)^2 \\
 &= \frac{1}{(m-1)m^2} \sum_{i=1}^m \left[(m-1)x_i - \sum_{j \neq i} x_j \right]^2 \\
 &= \frac{1}{(m-1)m^2} \sum_{i=1}^m \left[(m-1)^2 x_i^2 + \sum_{j \neq i} x_j^2 - 2(m-1)x_i \sum_{j \neq i} x_j + 2 \sum_{i \neq j} x_i x_j \right] \\
 &= \frac{1}{(m-1)m^2} \left[m(m-1) \sum_{i=1}^m x_i^2 - 2m \sum_{i \neq j} x_i x_j \right] \\
 &= \frac{1}{m} \sum_{i=1}^m x_i^2 - \frac{2}{m(m-1)} \sum_{i \neq j} x_i x_j, \tag{A.1}
 \end{aligned}$$

then the expectation of $(\text{rms})^2$ is given by

$$\begin{aligned}
 \langle (\text{rms})^2 \rangle &= \frac{1}{m} \sum_{i=1}^m \langle x_i^2 \rangle - \frac{2}{m(m-1)} \sum_{i \neq j} \langle x_i \rangle \langle x_j \rangle \\
 &= \langle x_i^2 \rangle - (\langle x_i \rangle)^2 \\
 &= \text{Var}(x) \\
 &= \lambda, \tag{A.2}
 \end{aligned}$$

where $\text{Var}(x)$ is the variance of $x(i)$. Thus, we obtain that for a Poisson counts series $x(i)$, the expectation of $(\text{rms})^2$ is λ .

Monte Carlo simulations are done using the counts series under Poisson processes to verify the above analytic result. The parameter λ is set from the range $[0.02, 2]$. For every λ , a Poisson count series of 10^5 data points with the parameter λ is produced. The counts series is divided into k segments and in each segment, there are m data points. The $(\text{rms})^2$ for each segment is calculated, averaged for all segments, and compared with λ , as shown in Figure A.1. For comparison, the rms for each segment is calculated, averaged and compared with $\sqrt{\lambda}$, as shown in Figure A.2. We conclude that for a Poisson series, $\langle (\text{rms})^2 \rangle$ is an unbiased estimator of λ ; however $\langle \text{rms} \rangle$ is not an unbiased estimator of $\sqrt{\lambda}$.

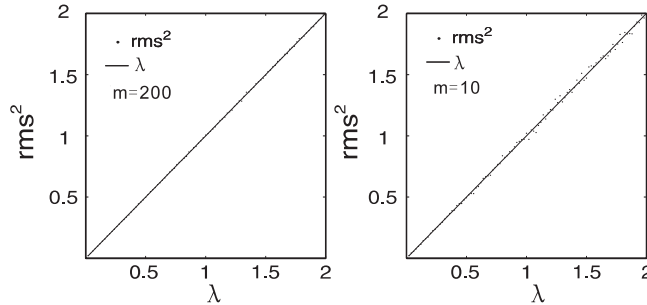


Fig. A.1 Relationship between $(\text{rms})^2$ and flux for counts series under Poisson processes. *Dots* are for $(\text{rms})^2$. *Lines* are for $(\text{rms})^2 = \lambda$.

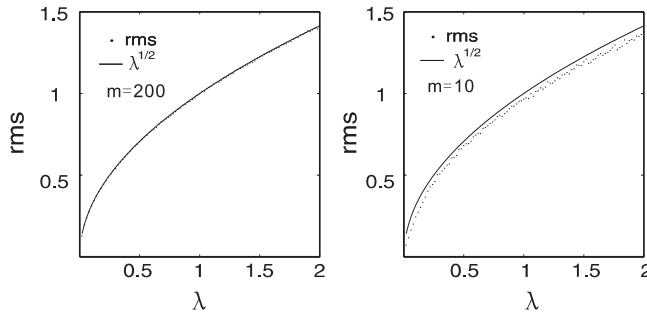


Fig. A.2 Relationship between rms and flux for counts series under Poisson processes. *Dots* are for rms. *Lines* are for $\text{rms} = \sqrt{\lambda}$.

References

- Abramowicz, M. A., & Kluźniak, W. 2001, *A&A*, 374, L19
 Belloni, T., Colombo, A. P., Homan, J., et al. 2002, *A&A*, 390, 199
 Corbel, S., Fender, R. P., Tzioumis, A. K., et al. 2002, *Science*, 298, 196
 Dubath, P., Revnivtsev, M., Goldoni, P., et al. 2003, *IAU Circ.*, 8100
 Feng, H., Li, T. P., & Zhang, S. N. 2004, *ApJ*, 606, 424
 Hannikainen, D., Wu, K., Cambell-Wilson, D., Hunstead, R., et al. 2001, in *Exploring the Gamma-Ray Universe*, ed. B. Battrick (ESA SP-459) (Noordwijk: ESA), 291

- Homan, J., Wijnands, R., van der Klis, M., et al. 2001, *ApJS*, 132, 377
- Kaaret, P., Corbel, S., Tomsick, J., et al. 2003, *ApJ*, 582, 945
- Li, T. P. 2001, *Chin. J. Astron. Astrophys.* 1, 313
- Li, T. P., & Muraki, Y. 2002, *ApJ*, 578, 374
- Miller, J. M., et al. 2001, *ApJ*, 563, 928
- Orosz, J. A., Groot, P. J., van der Klis, M., et al. 2002, *ApJ*, 568, 845
- Remillard & McClinoock. 2006, *ARA&A*, 44, 49
- Rodriguez, J., Corbel, S., & Tomsick, J. 2003, *ApJ*, 595, 1032
- Smith, D. A., Levine, A. M., Remillard, R., & Fox, D. 2000, *IAU Circ.* 7399
- Sobczak, G. J., McClintock, J. E., Remillard, R. A., et al. 1999, *ApJ*, 517, L121
- Sunyaev, R., & Revnivtsev, M. 2000, *A&A*, 358, 617
- Tomsick, J., Corbel S., & Karret P. 2001a, *ApJ*, 563, 229
- Tomsick, J., Smith, E., Swank, J., et al. 2001b, *IAU Circ.* 7575
- Uttley, P., McHardy, I. M., & Vaughan, S. 2005, *MNRAS*, 359, 345
- Zhang, S. N. 2006, Invited Discourse, the 26th IAU General Assembly, Prague, Czech Republic, (astro-ph/0702246)